Journal of Clinical and Translational Hepatology **2025** vol. 13(5) | 385–394
DOI: 10.14218/JCTH.2025.00007

Original Article

FTO Promotes Hepatocellular Carcinoma Progression by Mediating m6A Modification of BUB1 and Targeting TGF-βR1 to Activate the TGF-β Signaling Pathway

Lin Zhang[1,2#], Li Gan[3#], Yuru Lin[1], Zhechuan Mei[1*] and Shengtao Liao[1*]

[1]*Department of Gastroenterology, The Second Affiliated Hospital of Chongqing Medical University, Chongqing, China;* [2]*Department of Gastroenterology, Chongqing Jiangjin Central Hospital, Chongqing, China;* [3]*Department of Anatomy, and Laboratory of Neuroscience and Tissue Engineering, Basic Medical College, Chongqing Medical University, Chongqing, China*

Received: January 03, 2025 | **Revised:** March 01, 2025 | **Accepted:** March 17, 2025 | **Published online:** April 18, 2025

Abstract

Background and Aims: Fat mass and obesity-associated protein (FTO) has been linked to various cancers, though its role in hepatocellular carcinoma (HCC) remains unclear. This study aimed to investigate FTO expression, its clinical relevance, functional role in HCC progression, and the underlying molecular mechanisms. ***Methods:*** Quantitative reverse-transcription polymerase chain reaction and immunohistochemical analysis were used to assess FTO expression in HCC. Functional assays, including proliferation, invasion, and epithelial-mesenchymal transition studies, were conducted using HCC cell lines with FTO knockdown. N6-methyladenosine (m6A) RNA immunoprecipitation and RNA stability assays further elucidated the role of FTO in BUB1 mRNA methylation and stability. Co-immunoprecipitation studies were employed to confirm the interaction between BUB1 and TGF-βR1. *In vivo* studies in nude mice were conducted to evaluate tumor growth following FTO knockdown. ***Results:*** FTO was significantly upregulated in HCC tissues compared to normal liver tissues, with higher expression observed in advanced tumor-node-metastasis stages and metastatic HCC. Elevated FTO correlated with poor overall survival in patients. Silencing FTO decreased HCC cell proliferation, colony formation, invasion, epithelial-mesenchymal transition, and tumor growth in nude mice. Mechanistically, FTO downregulation led to increased m6A modification of BUB1 mRNA, thereby promoting its degradation via the YTH domain family 2-dependent pathway and reducing BUB1 protein levels. Additionally, BUB1 physically interacted with TGF-βR1, activating downstream TGF-β signaling. ***Conclusions:*** FTO is overexpressed in HCC and is associated with poor clinical outcomes. Mechanistically, FTO promotes HCC progression by stabilizing BUB1 mRNA through an m6A-YTH domain family 2–dependent pathway, which activates TGF-β signaling. Targeting the FTO–BUB1–TGF-βR1 regulatory network may offer a promising therapeutic strategy for HCC.

Citation of this article: Zhang L, Gan L, Lin Y, Mei Z, Liao S. FTO Promotes Hepatocellular Carcinoma Progression by Mediating m6A Modification of BUB1 and Targeting TGF-βR1 to Activate the TGF-β Signaling Pathway. J Clin Transl Hepatol 2025;13(5):385–394. doi: 10.14218/JCTH.2025.00007.

Introduction

Hepatocellular carcinoma (HCC) is a primary malignancy of the liver and represents a significant global health burden, ranking among the leading causes of cancer-related deaths worldwide.[1,2] The incidence of HCC is closely linked to chronic liver diseases, such as fibrosis and cirrhosis, which often result from prolonged hepatitis B or hepatitis C infections, alcohol abuse, and non-alcoholic fatty liver disease.[3,4] Despite advancements in surgical resection, locoregional therapies, and targeted molecular drugs, the overall survival rate of HCC patients remains suboptimal, highlighting the critical need for new biomarkers and targeted therapies to improve patient outcomes.[5,6]

In recent years, epitranscriptomic modifications, particularly N6-methyladenosine (m6A) on mRNA, have emerged as pivotal regulators of gene expression in cancer biology.[7–9] The dynamic nature of m6A modification is governed by "writers" (methyltransferases such as METTL3 and METTL14), "erasers" (demethylases including fat mass and obesity-associated protein (FTO) and ALKBH5), and "readers" (m6A recognition proteins such as YTH domain family (YTHDF) members: YTHDF1, YTHDF2, and YTHDC1/2).[10,11] Through these regulators, m6A influences mRNA stability, translation efficiency, and localization.[12] Accordingly, alterations in m6A regulators have been implicated in cancer initiation, progression, and metastasis.[13,14]

FTO is one of the first m6A demethylases identified. Initial studies on FTO focused on its role in metabolism and obesity, but further research has revealed its involvement in various pathophysiological processes, including carcinogenesis.[15] Elevated FTO expression has been observed in several malignancies, where it can enhance tumor growth, cell prolifera-

Keywords: Hepatocellular carcinoma; FTO; BUB1; TGF-βR1; m6A methylation; TGF-β signaling.

[#]Contributed equally to this work.

[*]**Correspondence to:** Shengtao Liao and Zhechuan Mei, Department of Gastroenterology, The Second Affiliated Hospital of Chongqing Medical University, No. 74 Linjiang Road, Yuzhong District, Chongqing 400010, China. ORCID: https://orcid.org/0009-0003-3150-7840 (SL). E-mail: jianghe@cqmu.edu.cn (SL) and meizhechuan@cqmu.edu.cn (ZM).

tion, and metastatic potential.[16] In HCC, emerging evidence supports a role for FTO as a critical oncogenic factor,[17,18] although the exact mechanisms by which FTO promotes HCC progression remain only partially understood.

In this study, we found that one downstream target of FTO in HCC is BUB1 (budding uninhibited by benzimidazoles 1), a key component of the mitotic checkpoint system. BUB1 encodes a serine/threonine kinase that plays essential roles in chromosome alignment and segregation during mitosis.[19] Aberrant BUB1 expression has been reported in various cancers, including HCC, and is often associated with poor prognosis.[20,21] However, the detailed molecular relationship between FTO and BUB1, involving m6A post-transcriptional regulation, has not been clearly delineated.

Further complexity arises from the cross-talk between BUB1 and TGF-β signaling. The TGF-β (transforming growth factor beta) pathway is integral to cell proliferation, differentiation, and survival, often exhibiting tumor-suppressor activity in early-stage tumors but paradoxically promoting invasion and metastasis in later stages of tumorigenesis.[22,23] The TGF-β receptor, TGF-βR1, along with its downstream effectors—such as SMAD2 and SMAD3—coordinates these biological responses.[24] Dysregulation of TGF-β signaling is frequently observed in advanced HCC and correlates with increased migration, invasion, and epithelial-mesenchymal transition (EMT).[25]

A recent study suggests that BUB1 binds to TGF-βR1, promoting its heterodimerization with TGF-βR2, which activates TGF-β signaling and regulates cellular biological functions.[26] Nonetheless, how FTO-mediated m6A regulation of BUB1 mRNA integrates with TGF-β-driven oncogenic programs remains an active area of investigation. A critical understanding of these interconnected pathways may lead to novel therapeutic options for aggressive liver cancers.

Methods

Human tissue collection

HCC tissues and adjacent normal liver tissues were collected from 50 patients undergoing surgical resection at The Second Affiliated Hospital of Chongqing Medical University. Among these, 31 cases were classified as tumor-node-metastasis (TNM) stage I-II, 19 cases as TNM stage III-IV, and 12 cases presented with distant metastasis. None of the patients had received chemotherapy or radiotherapy prior to surgery. All specimens were histopathologically verified. Tissue samples were immediately snap-frozen in liquid nitrogen and stored at −80°C for subsequent assays. Written informed consent was obtained from all participants, and this study was approved by the Ethics Committee of The Second Affiliated Hospital of Chongqing Medical University (2021[152]).

Cells, cell culture, and transfection

The human HCC cell lines Hep3b and MHCC97H were obtained from the Cell Bank of the Chinese Academy of Sciences (Shanghai, China). Cells were maintained in Dulbecco's Modified Eagle Medium (DMEM; Gibco, Thermo Fisher Scientific, USA) supplemented with 10% fetal bovine serum (FBS; Gibco, Thermo Fisher Scientific, USA) and 1% penicillin-streptomycin (HyClone, Cytiva, USA) at 37°C in a humidified incubator with 5% CO_2. For knockdown of target genes (FTO, YTHDF2, and BUB1), short hairpin RNAs were purchased from GenePharma (Shanghai, China). For overexpression experiments, full-length coding sequences were cloned into pcDNA3.1 vectors (Invitrogen, Thermo Fisher Scientific, USA). Transfections were performed using Lipofectamine 3000 (Invitrogen, Thermo Fisher Scientific, USA) according to the manufacturer's protocol.[27] Stably transfected cell lines were selected and maintained in medium containing 2 μg/mL puromycin (Sigma-Aldrich, Merck, Germany) when applicable.

Database analysis

FTO expression levels in HCC were analyzed using data from The Cancer Genome Atlas (TCGA).[28] Expression profiles and corresponding clinical information were downloaded from the Genomic Data Commons Data Portal. Differential expression between tumor and normal tissues was computed, with a p-value < 0.05 considered statistically significant.

RNA sequencing

Total RNA was extracted using TRIzol reagent (Invitrogen) from cells treated with sh-FTO or sh-NC (negative control). RNA quality was assessed using an Agilent 2100 Bioanalyzer (Agilent Technologies). Libraries were prepared using the NEBNext Ultra RNA Library Prep Kit for Illumina (New England Biolabs) according to the manufacturer's instructions. Sequencing was performed on an Illumina platform (HiSeq or NovaSeq) to generate 150-bp paired-end reads. Differentially expressed genes were identified with $|\log_2(\text{fold change})| \geq 1$ and $p < 0.05$, and KEGG pathway enrichment analysis was conducted.[29]

Cell counting kit-8 (CCK-8) assay

Cell proliferation was measured using the CCK-8 (Dojindo, Japan). Briefly, transfected Hep3b or MHCC97H cells were seeded in 96-well plates. At designated time points (Day 1, 2, 3, 4), 10 μL of CCK-8 solution was added to each well and incubated for 2 h at 37°C. Optical density values at 450 nm were recorded using a microplate reader (Bio-Rad, USA).[30] Each experiment was performed in triplicate.

Colony formation assay

For colony formation analysis,[31] 500 transfected cells were plated in six-well plates and maintained in complete medium for 10–14 days. The medium was changed every three days. Colonies were fixed in 4% paraformaldehyde (Sigma-Aldrich, USA) for 15 min and stained with 0.1% crystal violet. Visible colonies were counted under a microscope. Each experiment was performed at least in triplicate.

Transwell invasion assay

Cell invasion was evaluated using a Transwell system (Corning, USA) coated with Matrigel (Corning, USA).[32] Matrigel was diluted 1:8 in serum-free DMEM, coated onto membranes, and polymerized at 37°C for 1 h prior to cell seeding. Briefly, transfected cells in serum-free medium were placed in the upper chamber. Complete medium containing 10% FBS served as a chemoattractant in the lower chamber. After 24 h of incubation, non-invading cells were removed with a cotton swab. Cells that had invaded through the membrane were fixed with 4% paraformaldehyde (Sigma-Aldrich, USA), stained with 0.1% crystal violet (Sigma-Aldrich, USA), and counted in five randomly selected fields under an inverted microscope.

Real-time quantitative polymerase chain reaction (qPCR)

Total RNA was extracted using TRIzol reagent (Invitrogen, USA), and 1 μg of RNA was reverse-transcribed using a Pri-

meScript RT reagent kit (Takara, Japan) according to the manufacturer's instructions. Quantitative real-time qPCR was performed with SYBR Green PCR Master Mix (Applied Biosystems, USA) on a StepOnePlus Real-Time PCR System (Applied Biosystems, USA). The relative expression of target genes was determined using the $2^{-\Delta\Delta Ct}$ method, with GAPDH as an internal control.[33]

Western blotting

Cells or tissues were lysed in RIPA buffer (Beyotime, China) containing protease and phosphatase inhibitors (Roche, Switzerland). Protein concentrations were measured using the BCA Protein Assay Kit (Thermo Fisher Scientific, USA). Equal amounts (30 μg) of proteins were loaded onto SDS-PAGE gels (Bio-Rad, USA) and transferred to PVDF membranes (Millipore, USA). Membranes were blocked with 5% nonfat milk in TBST, then incubated with primary antibodies overnight at 4°C. After washing, membranes were incubated with HRP-conjugated secondary antibodies (Thermo Fisher Scientific, USA) for 1 h at room temperature. Protein bands were visualized using an ECL detection kit (Bio-Rad, USA) and quantified with ImageJ software.[34] β-actin served as an internal loading control.

Co-immunoprecipitation

To examine BUB1–TGF-βR1 interactions, co-immunoprecipitation assays were conducted.[35] Hep3b cells were lysed in immunoprecipitation buffer (Beyotime, China) supplemented with protease inhibitors. Lysates (500–1,000 μg of total protein) were precleared with protein A/G agarose beads (Thermo Fisher Scientific, USA) for 2 h at 4°C. Subsequently, the supernatant was incubated with specific antibodies: anti-TGF-βR1 (2 μg per 1 mL lysate), anti-BUB1 (2 μg per 1 mL lysate), or control IgG (2 μg per 1 mL lysate), overnight at 4°C with gentle rotation. The immunocomplex was captured by fresh protein A/G agarose beads for an additional 2 h. Beads were then washed three times with immunoprecipitation buffer, and bound proteins were eluted by boiling in the SDS sample buffer. Eluted proteins were subjected to SDS-PAGE and Western blotting as described above.

RNA immunoprecipitation (RIP)

RIP was performed using the Magna RIP Kit (Millipore, USA) to investigate RNA–YTHDF2 interactions.[36] Cells were lysed in RIP lysis buffer, and lysates were incubated with magnetic beads conjugated to the specific antibody or control IgG. After washing, RNA was extracted from the immunocomplexes using TRIzol (Invitrogen, USA) and subjected to qRT-PCR for BUB1 detection. The enrichment of a specific transcript in RIP samples was analyzed relative to the input.

RNA stability assays

For RNA stability measurements,[37] actinomycin D (ActD; Selleck Chemicals, USA) was added to the culture medium at a final concentration of 5 μg/mL. Cells were harvested at multiple time points (0, 2, 4, 6 h) following ActD treatment. Total RNA was isolated at each time point, and the levels of BUB1 mRNA were quantified by qRT-PCR.

Immunohistochemistry

Paraffin-embedded tissue sections (4 μm) from clinical samples were deparaffinized, rehydrated, and subjected to antigen retrieval. Endogenous peroxidases were blocked with 3% H_2O_2, and nonspecific binding was blocked using 5% normal goat serum. Slides were incubated overnight at 4°C with anti-FTO followed by an HRP-linked secondary antibody (Thermo Fisher Scientific, USA) for 1 h at room temperature. Signal development was achieved using a DAB substrate kit (Vector Labs, USA), and hematoxylin counterstaining was performed. Staining intensity was evaluated by two independent pathologists who were blinded to the experimental conditions.

Methylated RNA immunoprecipitation (MeRIP)-qPCR

MeRIP was carried out to assess m6A modification levels of BUB1 using the Magna MeRIP m6A Kit (Millipore, USA).[38] Briefly, 200 μg of total RNA was fragmented to an average length of ~200 nt by incubation with fragmentation buffer. The sample was then immunoprecipitated with an anti-m6A antibody conjugated to Protein A/G beads (Thermo Fisher Scientific, USA). Eluted RNA was purified, and the relative enrichment of specific transcripts was quantified via qRT-PCR. IgG was used as the negative control. Results were normalized to input RNA.

Immunofluorescence

Cells grown on coverslips were fixed with 4% paraformaldehyde for 15 min, permeabilized with 0.1% Triton X-100, and blocked with 5% normal donkey serum (Abbkine, China) for 1 h at room temperature. Anti-Ki67 antibody was incubated at 4°C overnight. After PBS washes, coverslips were incubated with appropriate fluorescence-conjugated secondary antibodies (Thermo Fisher Scientific, USA) for 1 h at room temperature and stained with DAPI (Beyotime, China) to visualize nuclei.[39] Immunofluorescence images were captured using a confocal laser scanning microscope (Zeiss LSM 710).

In vivo tumor xenograft model

Animal experiments were performed in accordance with the guidelines of the Institutional Animal Care and Use Committee at The Second Affiliated Hospital of Chongqing Medical University. Four- to six-week-old BALB/c nude mice were obtained from the Experimental Animal Center of Chongqing Medical University. For subcutaneous xenografts, ~2×10^6 Hep3b cells (stably transfected with sh-FTO or control sh-NC) were suspended in 100 μL of a Matrigel/PBS mixture and injected into the flank of each mouse (n = 8 per group). Tumor dimensions were measured every seven days using digital calipers. Tumor volume was calculated using the formula: $V = (\text{length} \times \text{width}^2)/2$.[40] Mice were sacrificed at the endpoint as determined by the Institutional Animal Care and Use Committee humane criteria, and tumor tissues were excised for further analyses.

Statistical analysis

Data are presented as mean ± standard deviation from at least three independent experiments. All data were first tested for normal distribution using the Shapiro-Wilk test. For normally distributed data, comparisons between two groups were performed using Student's t-test, while non-normally distributed data were analyzed using the Mann-Whitney U test. Differences among multiple groups were assessed using one-way ANOVA followed by Tukey's post hoc test. Correlations between gene expression levels were analyzed using Pearson's correlation coefficient. Survival curves were generated using Kaplan-Meier analysis with the log-rank test. Patients were categorized into high or low FTO expression groups (n = 25 each) based on median FTO mRNA levels from qRT-PCR. Statistical significance was defined as $p < 0.05$. GraphPad Prism 10.1.2 (GraphPad Software) was used for data processing and visualization.

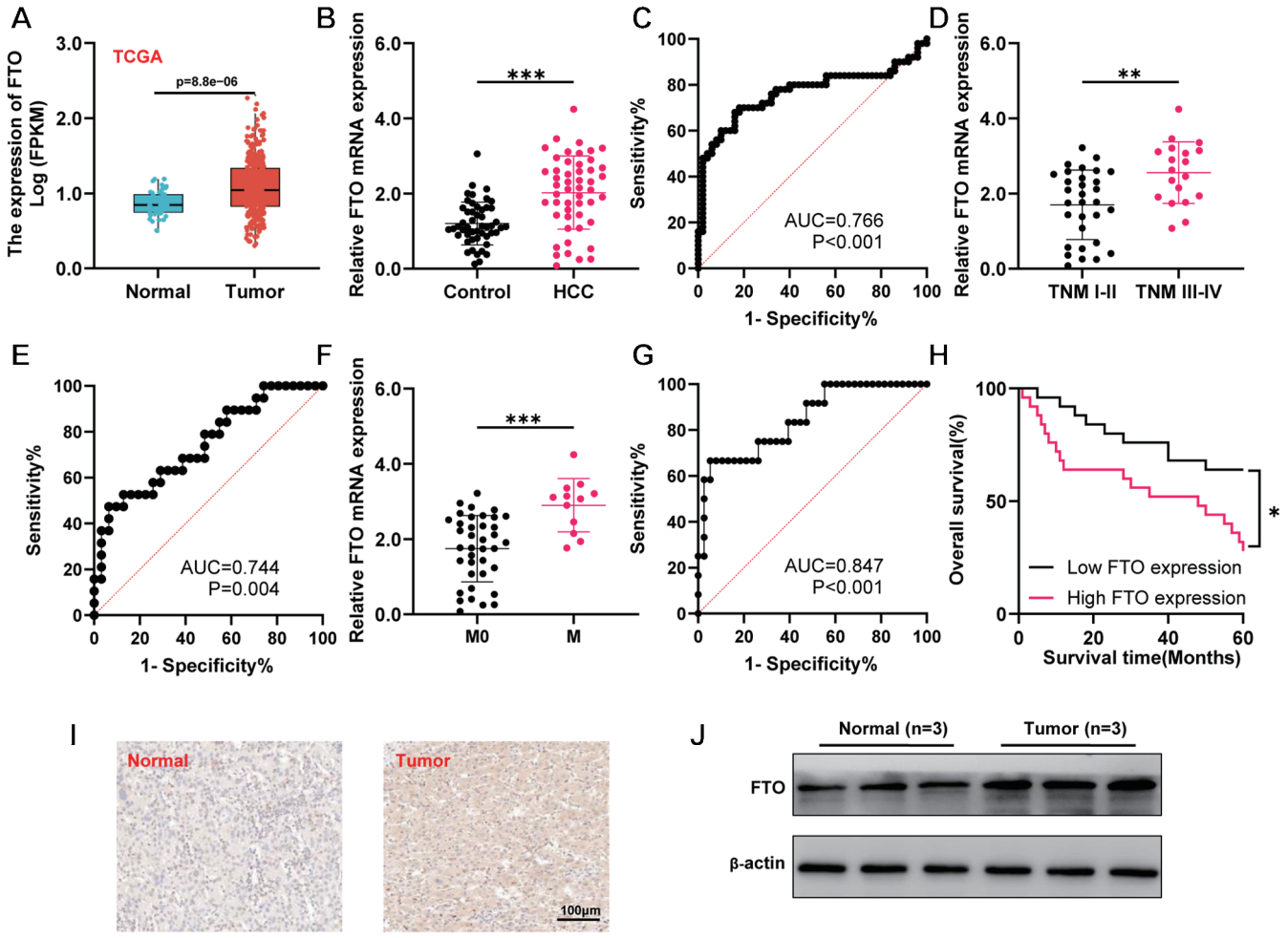

Fig. 1. FTO expression in HCC and its relationship with clinical outcomes. (A) Box plot of FTO expression levels in HCC tissues and normal liver tissues from The Cancer Genome Atlas (TCGA) database. (B) qRT-PCR analysis of FTO mRNA levels in HCC tissues compared with adjacent normal tissues. (C) ROC curve displaying the diagnostic performance of FTO in distinguishing HCC tissues from normal tissues. (D) FTO expression levels in patients with different TNM stages of HCC. (E) ROC curve for FTO in differentiating between early-stage and advanced-stage HCC. (F) FTO mRNA levels in HCC patients with and without metastasis. (G) ROC curve analysis of FTO expression for discriminating between HCC patients with and without metastasis. (H) Kaplan-Meier survival analysis of HCC patients stratified by high vs. low FTO expression. (I) Representative images of immunohistochemical staining for FTO protein in HCC and adjacent normal tissues. (J) Western blot analysis of FTO protein levels in three pairs of HCC and matched normal samples. *$p < 0.05$, **$p < 0.01$, ***$p < 0.001$. Data are expressed as mean ± standard deviation. HCC, hepatocellular carcinoma; qRT-PCR, quantitative reverse transcription polymerase chain reaction; ROC, receiver operating characteristic; TNM, tumor-node-metastasis; FTO, fat mass and obesity-associated.

Results

High expression of FTO in HCC associated with poor prognosis

To evaluate the expression pattern and clinical relevance of FTO in HCC, publicly accessible data from TCGA were analyzed. In these datasets, FTO was found to be significantly upregulated in HCC tissues compared to normal liver tissues (Fig. 1A). Elevated FTO expression in paired human HCC specimens and adjacent normal controls was further confirmed using qRT-PCR (Fig. 1B). Receiver operating characteristic (ROC) curve analysis showed an area under the curve (AUC) of 0.766 for FTO, suggesting a strong ability to distinguish HCC from normal tissues (Fig. 1C). When HCC samples were stratified according to TNM stage, FTO expression exhibited a progressive increase in advanced disease stages (Fig. 1D), which was supported by an additional ROC analysis (Fig. 1E). Patients with metastatic HCC also demonstrated higher levels of FTO (Fig. 1F), and this finding was validated by an ROC curve (Fig. 1G). Furthermore, a Kaplan-Meier survival analysis indicated that patients with elevated FTO had a significantly reduced overall survival rate (Fig. 1H). Immunohistochemistry staining detected stronger FTO signals in tumor tissues than in matched adjacent tissues (Fig. 1I), and Western blot analysis reinforced these observations at the protein level (Fig. 1J). Taken together, these results revealed that FTO was highly expressed in HCC and was associated with poor clinical outcomes.

Knockdown of FTO inhibited proliferation, invasion, and EMT in HCC cells

To investigate the functional importance of FTO in HCC progression, small hairpin RNAs were employed to reduce FTO in Hep3b and MHCC97H cell lines. Western blot and qRT-PCR analysis confirmed a marked reduction in FTO protein expression in sh-FTO cells compared to negative control (sh-

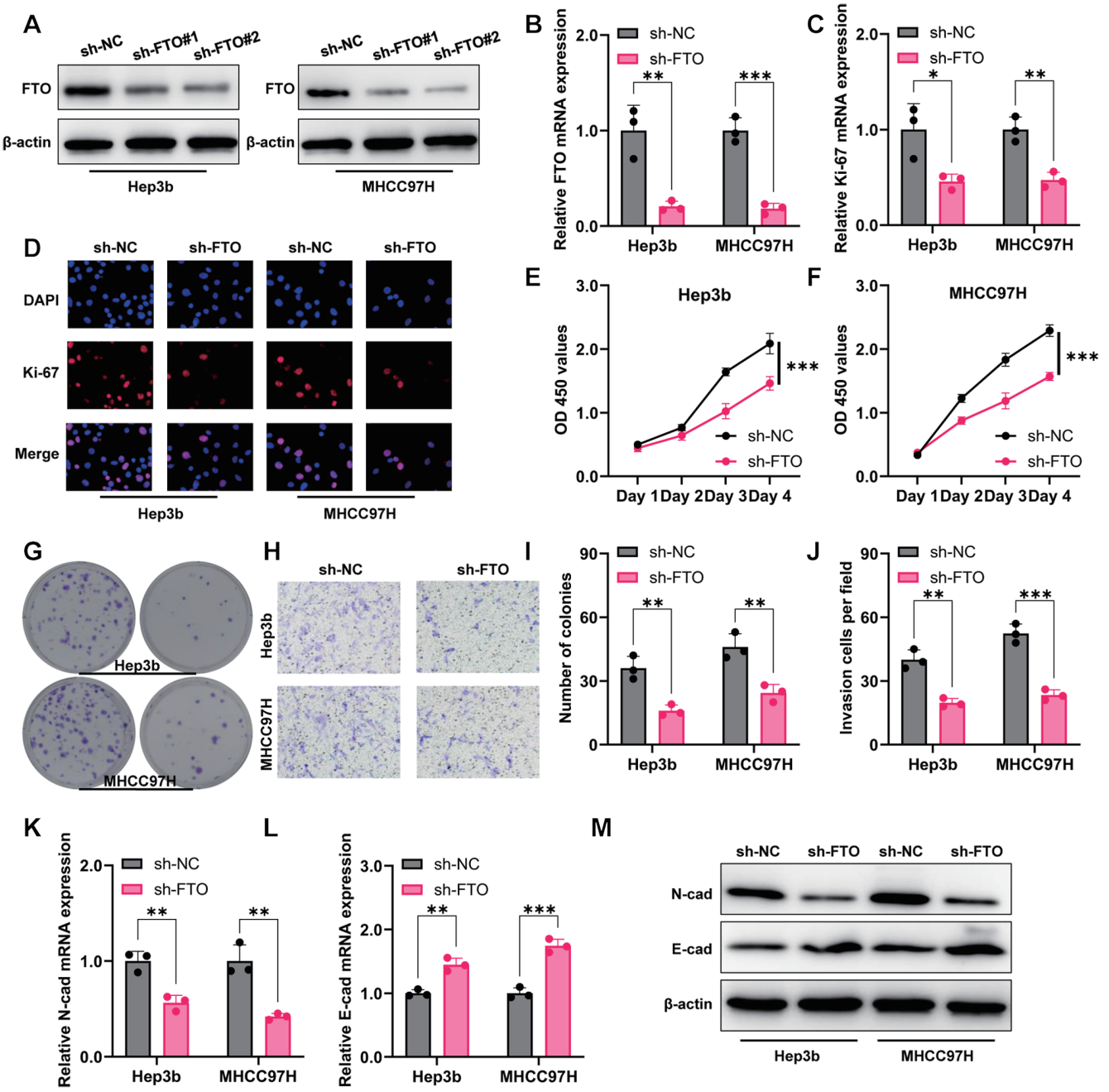

Fig. 2. Effects of FTO knockdown on HCC cells. (A) and (B) Western blot analysis of FTO levels in Hep3b and MHCC97H cells transduced with sh-FTO or sh-NC. (C) and (D) Immunofluorescence staining for Ki-67 in Hep3b and MHCC97H cells transduced with sh-FTO or sh-NC. (E) and (F) CCK-8 assays measuring the proliferation of Hep3b and MHCC97H cells transduced with sh-FTO or sh-NC. (G) and (I) Colony formation assays of Hep3b and MHCC97H cells transduced with sh-FTO or sh-NC. (H) and (J) Transwell invasion assays measuring the invasive capacity of Hep3b and MHCC97H cells transduced with sh-FTO or sh-NC. (K) and (L) qRT-PCR analysis of E-cadherin and N-cadherin mRNA levels in Hep3b and MHCC97H cells transduced with sh-FTO or sh-NC. (M) Western blot analysis of E-cadherin and N-cadherin proteins in Hep3b and MHCC97H cells transduced with sh-FTO or sh-NC. * $p < 0.05$, ** $p < 0.01$, *** $p < 0.001$. Data are expressed as mean ± standard deviation. HCC, Hepatocellular Carcinoma; sh-FTO, short hairpin RNA targeting FTO; sh-NC, short hairpin RNA negative control; CCK-8, Cell Counting Kit-8; qRT-PCR, quantitative reverse transcription polymerase chain reaction; FTO, fat mass and obesity-associated.

NC) cells (Fig. 2A and B). When FTO levels were decreased, Ki-67 expression was lower than in controls, suggesting a loss of proliferative capacity (Fig. 2C and D). CCK-8 assays showed that proliferation was diminished in sh-FTO–treated cells at multiple time points (Fig. 2E and F). Colony formation assays also demonstrated that fewer colonies were formed by FTO-depleted cells (Fig. 2G and I). In invasion assays, reduced FTO expression led to decreased invasive behavior in both Hep3b and MHCC97H cells (Fig. 2H and J). Moreover, EMT-related markers were evaluated by qRT-PCR and Western blot. E-cadherin was found to be elevated, whereas N-cadherin was diminished at both the mRNA and protein levels

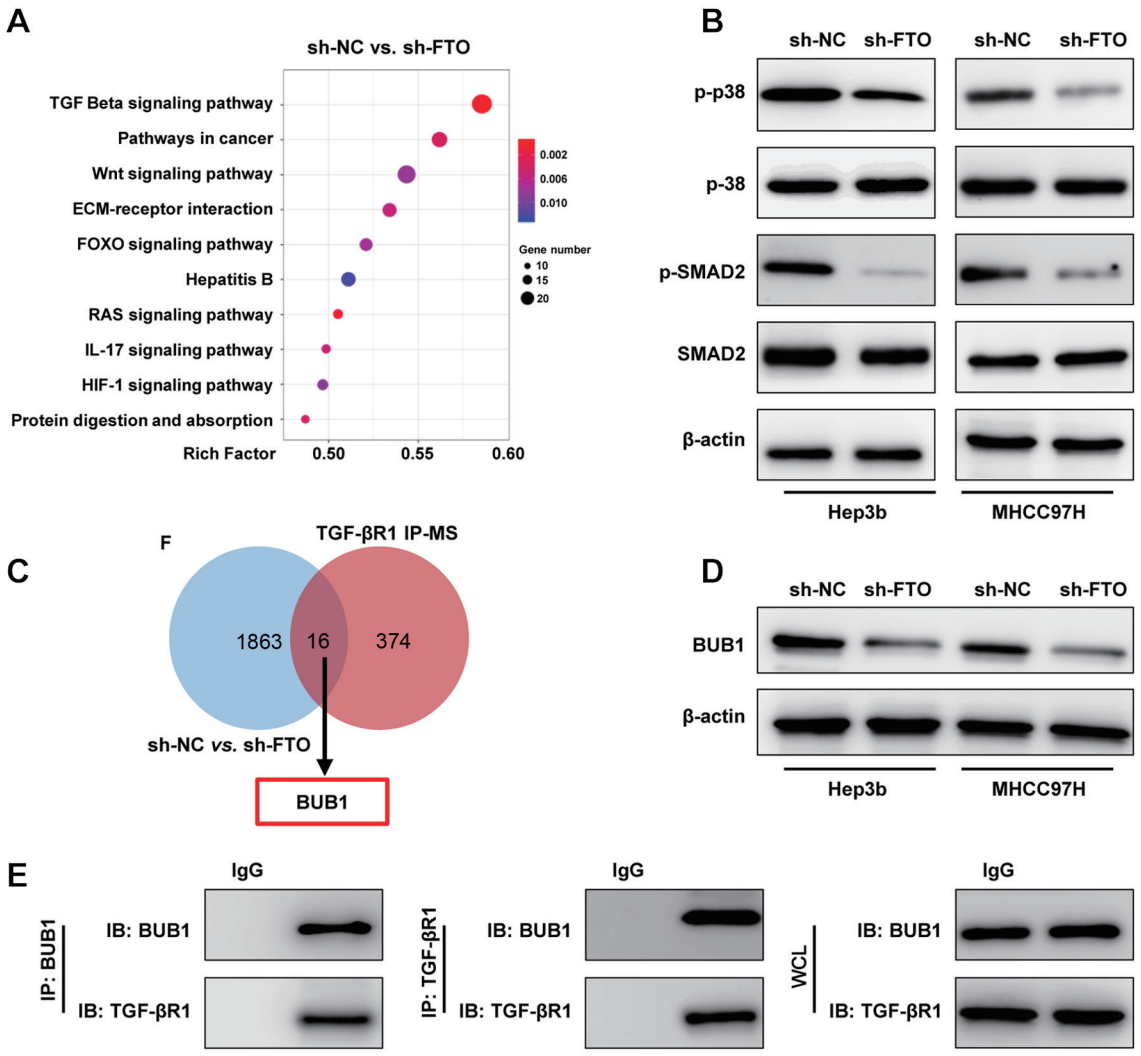

Fig. 3. BUB1 protein interacts with TGF-βR1. (A) KEGG pathway enrichment analysis of differentially expressed genes in Hep3b cells transduced with sh-FTO or sh-NC. (B) Western blot measurements of TGF-β–associated proteins in Hep3b and MHCC97H cells transduced with sh-FTO or sh-NC. (C) Venn diagram depicting the overlap between proteins altered by FTO knockdown and those immunoprecipitated with TGF-βR1. (D) Western blot analysis of BUB1 protein levels in Hep3b and MHCC97H cells transduced with sh-FTO or sh-NC. (E) Co-immunoprecipitation assay showing the interaction between BUB1 and TGF-βR1. Data are expressed as mean ± standard deviation. TGF-βR1, Transforming Growth Factor-β Receptor 1; KEGG, Kyoto Encyclopedia of Genes and Genomes; HCC, Hepatocellular Carcinoma; sh-FTO, short hairpin RNA targeting FTO; sh-NC, short hairpin RNA negative control; TGF-β, Transforming Growth Factor-β; FTO, fat mass and obesity-associated.

in sh-FTO cells (Fig. 2K, L, and M). These data indicated that the knockdown of FTO suppressed proliferation, invasion, and EMT in HCC cells.

BUB1 protein interacted with TGF-βR1

Subsequent analyses were performed to identify the potential downstream effectors of FTO in HCC. RNA sequencing data indicated that genes related to TGF-β signaling were among the most significantly altered after FTO knockdown (Fig. 3A). Consistently, levels of phosphorylated SMAD2 and phosphorylated p38 were reduced in sh-FTO cells, indicating downregulation of TGF-β pathway signaling (Fig. 3B). To further pinpoint factors involved in this pathway, TGF-βR1 was immunoprecipitated, followed by mass spectrometry, revealing an overlap of proteins that were differentially regulated by FTO knockdown (Fig. 3C). Among the intersection, BUB1 was identified as a significant target. In line with this finding, FTO knockdown reduced BUB1 protein levels (Fig. 3D). A subsequent co-immunoprecipitation assay demonstrated that BUB1 and TGF-βR1 formed a physical interaction (Fig. 3E), suggesting that BUB1 might be critical for TGF-βR1-mediated signaling in HCC cells.

FTO regulated BUB1 expression via an m6A-YTHDF2-dependent mechanism

Considering the role of FTO as an m6A demethylase, we hypothesized that FTO may increase BUB1 expression by modulating its mRNA methylation status. BUB1 mRNA was observed to be significantly higher in HCC tissues than in matched normal tissues (Fig. 4A), and its expression displayed a positive correlation with FTO (Fig. 4B). FTO inhibition via sh-FTO resulted in a marked decrease in both BUB1 mRNA and protein (Figs. 3D and 4C). To assess m6A levels on BUB1 mRNA following FTO knockdown, MeRIP was carried out in both the sh-NC and sh-FTO groups. The results revealed that m6A levels on BUB1 transcripts increased

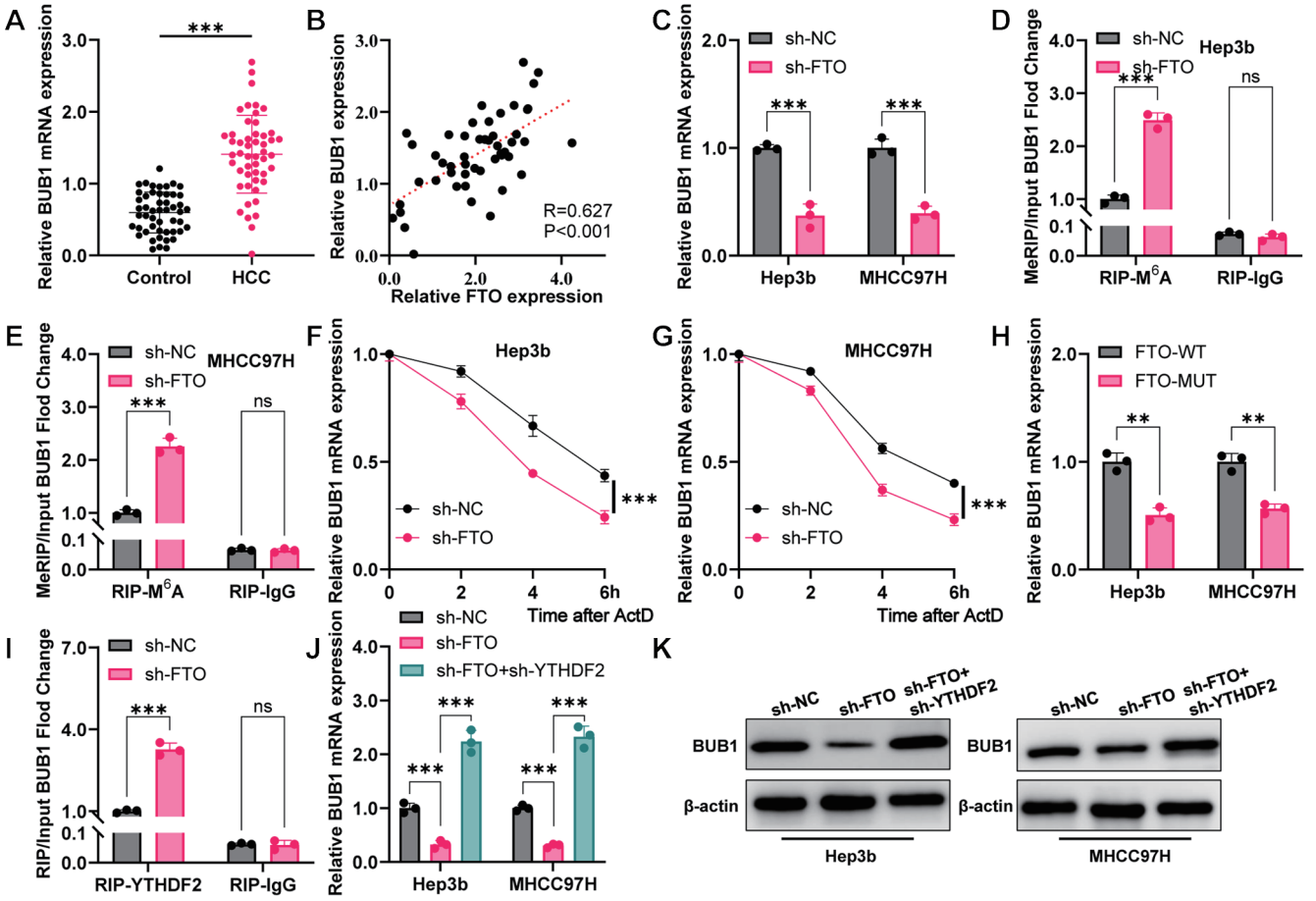

Fig. 4. FTO regulation of BUB1 expression via an m6A-YTHDF2-dependent mechanism (A) qRT-PCR analysis of BUB1 expression in HCC and adjacent normal tissues. (B) Correlation between FTO and BUB1 mRNA expression in HCC tissues. (C) qRT-PCR analysis of BUB1 mRNA levels in Hep3b and MHCC97H cells transduced with sh-FTO or sh-NC. (D) and (E) MeRIP assays measuring m6A enrichment on BUB1 mRNA in Hep3b and MHCC97H cells transduced with sh-FTO or sh-NC. (F) and (G) BUB1 mRNA stability assays using ActD in Hep3b and MHCC97H cells transduced with sh-FTO or sh-NC. (H) qRT-PCR analysis of BUB1 mRNA levels in Hep3b and MHCC97H cells overexpressing wild-type FTO (FTO-WT) or mutant FTO (FTO-MUT). (I) RIP analysis of YTHDF2 binding to BUB1 mRNA in Hep3b and MHCC97H cells transduced with sh-FTO or sh-NC. (J) qRT-PCR analysis of BUB1 levels in Hep3b and MHCC97H cells transduced with sh-NC, sh-FTO, and sh-FTO+sh-YTHDF2. (K) Western blot analysis of BUB1 protein levels in Hep3b and MHCC97H cells treated with sh-NC, sh-FTO, and sh-FTO+sh-YTHDF2. $^{**}p < 0.01$, $^{***}p < 0.001$. Data are expressed as mean ± standard deviation. HCC, Hepatocellular Carcinoma; m6A, N6-methyladenosine; qRT-PCR, quantitative reverse transcription polymerase chain reaction; sh-FTO, short hairpin RNA targeting FTO; sh-NC, short hairpin RNA negative control; MeRIP, Methylated RNA Immunoprecipitation; ActD, Actinomycin D; FTO-WT, wild-type FTO; FTO-MUT, mutant FTO; RIP, RNA Immunoprecipitation; sh-YTHDF2, short hairpin RNA targeting YTHDF2; FTO, fat mass and obesity-associated.

significantly when FTO was knocked down (Fig. 4D and E). Furthermore, RNA stability assays conducted in the presence of actinomycin D indicated a faster decay rate of BUB1 mRNA in FTO-silenced cells (Fig. 4F and G). Overexpression of wild-type FTO effectively elevated BUB1 transcript levels, whereas an enzymatically inactive FTO mutant did not (Fig. 4H). Moreover, RIP showed that YTHDF2, which targets m6A-marked RNAs for degradation, bound more robustly to BUB1 mRNA following FTO depletion (Fig. 4I). Partial rescue of BUB1 expression was achieved by concurrently knocking down YTHDF2 in FTO-silenced cells (Fig. 4J and K). These observations demonstrated that FTO sustained BUB1 expression via an m6A-YTHDF2-dependent mechanism.

FTO-mediated BUB1 activation of the TGF-β signaling pathway promotes HCC progression

Given that BUB1 physically interacted with TGF-βR1, further investigations were conducted to determine whether FTO modulated TGF-β signaling through BUB1. Overexpression of FTO in both Hep3b and MHCC97H cells enhanced BUB1 and Ki-67 expression (Fig. 5A and C), accompanied by increased phosphorylation of SMAD2 (Fig. 5B). Augmented proliferation, as assessed by the CCK-8 assay, was observed following FTO overexpression (Fig. 5D and E). Additionally, FTO overexpression reduced E-cadherin levels and increased N-cadherin levels (Fig. 5F and G), promoting cell invasion (Fig. 5H and I). However, simultaneous depletion of BUB1 (OE-FTO + sh-BUB1) counteracted these pro-tumor effects, implicating BUB1 as a key mediator of FTO-driven TGF-β-related oncogenesis (Fig. 5A–H). Finally, subcutaneous xenograft models in nude mice were used to determine the functional impact of FTO *in vivo*. Tumor volumes were significantly smaller in the sh-FTO groups compared to control animals (Fig. 5J and K). These findings suggest that FTO promotes HCC progression by facilitating BUB1-mediated TGF-β signaling and underscore the potential of targeting the FTO–BUB1–TGF-βR1 axis as a therapeutic strategy in liver cancer.

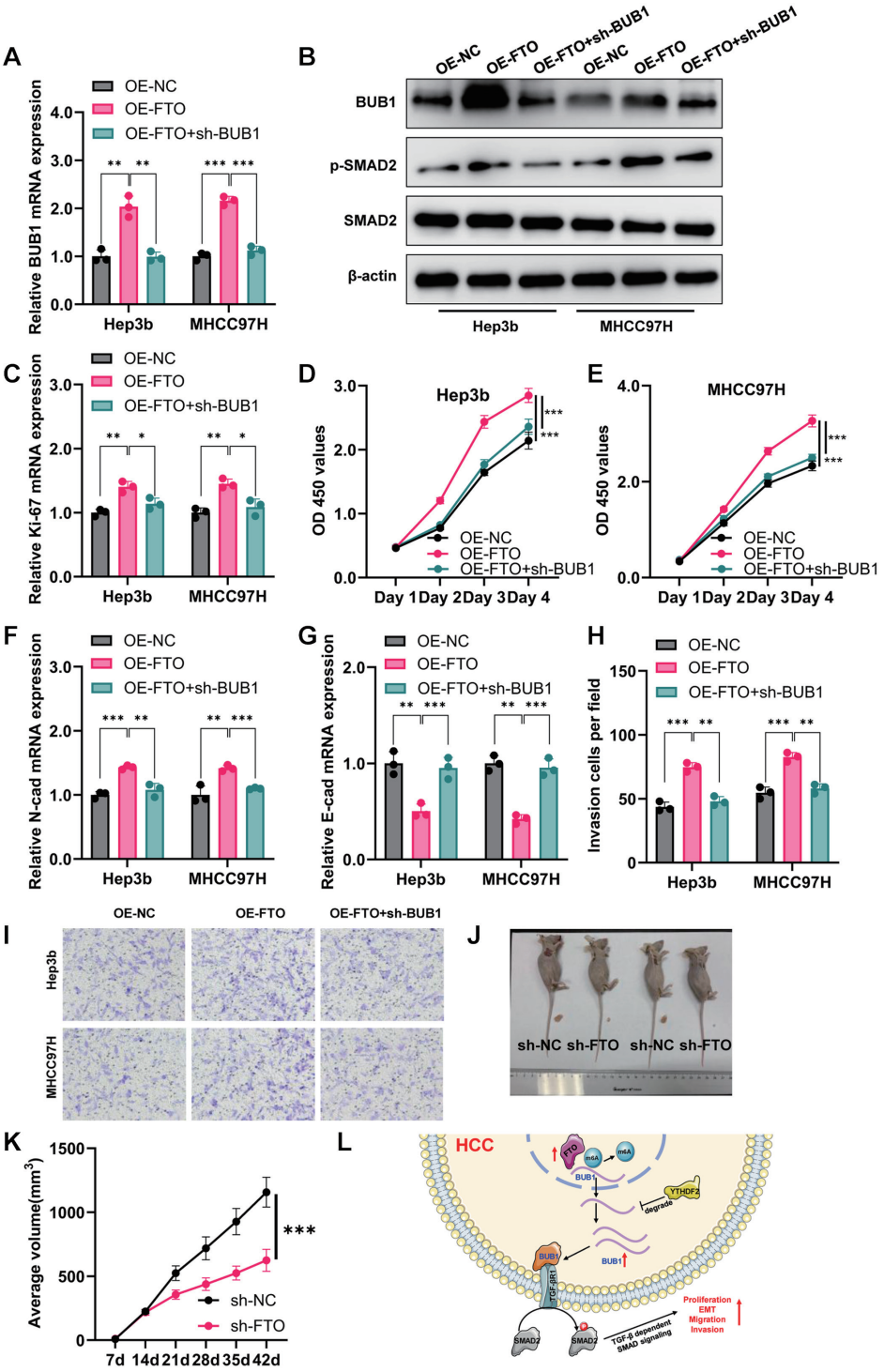

Fig. 5. Effects of FTO-mediated BUB1 activation on the TGF-β signaling pathway and HCC progression. (A) and (C) qRT-PCR analysis of BUB1 and Ki-67 expression in Hep3b and MHCC97H cells treated with OE-NC, OE-FTO, and OE-FTO+sh-BUB1. (B) Western blot analysis of BUB1, phosphorylated SMAD2, and SMAD2 protein levels in Hep3b and MHCC97H cells treated with OE-NC, OE-FTO, and OE-FTO+sh-BUB1. (D) and (E) CCK-8 assays measuring proliferation in Hep3b and MHCC97H cells with OE-NC, OE-FTO, and OE-FTO+sh-BUB1. (F) and (G) qRT-PCR analysis of E-cadherin and N-cadherin mRNA levels in Hep3b and MHCC97H cells treated with OE-NC, OE-FTO, and OE-FTO+sh-BUB1. (H) and (I) Transwell invasion assays measuring invasion ability in Hep3b and MHCC97H cells treated with OE-NC, OE-FTO, and OE-FTO+sh-BUB1. (J) and (K) Growth curves of subcutaneous xenograft tumors in nude mice injected with sh-FTO or sh-NC stable cell lines. (L) Schematic diagram illustrating the role of FTO-induced BUB1 upregulation in activating the TGF-β signaling pathway and promoting HCC progression, created with BioRender.com. * $p < 0.05$, ** $p < 0.01$, *** $p < 0.001$. Data are expressed as mean ± standard deviation. HCC, Hepatocellular Carcinoma; qRT-PCR, quantitative reverse transcription polymerase chain reaction; OE-NC, overexpression negative control; OE-FTO, overexpression of FTO; sh-BUB1, short hairpin RNA targeting BUB1; CCK-8, Cell Counting Kit-8; TGF-β, Transforming Growth Factor-β; sh-FTO, short hairpin RNA targeting FTO; sh-NC, short hairpin RNA negative control; FTO, fat mass and obesity-associated.

Discussion

Early detection and effective treatment for HCC remain significant clinical challenges, largely due to the tumor's heterogeneity and high metastatic propensity.[41,42] Epitranscriptomic mechanisms, including m6A modifications, have emerged as vital regulatory factors in various cancer types.[43] In this study, FTO was shown to be highly expressed in HCC and correlated with poorer clinical outcomes. Mechanistically, FTO elevated BUB1 expression by reducing m6A levels, thereby preventing BUB1 mRNA degradation through an m6A-YTHDF2-dependent pathway. Furthermore, BUB1 physically interacted with TGF-βR1, promoting TGF-β signaling and driving HCC progression (Fig. 5L).

FTO was initially studied for its association with obesity, with single nucleotide polymorphisms in the FTO locus significantly associated with body mass index.[44] After recognizing that FTO functions as an m6A demethylase, its oncogenic or tumor-suppressive roles have been explored.[45] Studies show that in certain tumors, FTO overexpression typically confers growth advantages, facilitating proliferation, self-renewal of cancer stem cells, and even resistance to chemotherapy.[46,47] Consistent with previous reports indicating an oncogenic role for FTO in colorectal cancer and melanoma,[48,49] our data validate FTO's function in promoting HCC cell proliferation, invasion, and EMT. Importantly, we identified BUB1—a key mitotic checkpoint kinase—as a novel direct target of FTO.

FTO likely executes its oncogenic functions through the demethylation of transcripts encoding pro-tumorigenic proteins, thereby stabilizing those mRNAs or enhancing their translation.[45] BUB1 appears to be one such transcript in HCC, mediated by the YTHDF2 reader protein. Ordinarily, YTHDF2 recognizes m6A-modified transcripts and promotes their degradation in processing bodies or stress granules.[50] However, when BUB1 transcripts contain fewer m6A marks due to elevated FTO activity, the efficiency of YTHDF2 binding and subsequent decay decreases, potentially leading to increased translation of BUB1 protein.

BUB1 is traditionally recognized for its central role in the mitotic spindle checkpoint.[51] In healthy cells, it prevents aneuploidy by halting the metaphase-to-anaphase transition until chromosomes are correctly aligned. Cancer cells often exploit or bypass these checkpoint pathways to accelerate cell cycle progression.[52] Hence, the aberrant elevation of BUB1 might confer a proliferative advantage and promote genomic instability—characteristics of aggressive tumor phenotypes.[53]

Our study adds depth to this perspective by demonstrating how BUB1 binds TGF-βR1 to enhance TGF-β–mediated oncogenic signaling. Although the TGF-β pathway can exhibit both tumor-suppressive and tumor-promoting functions, advanced-stage HCC generally exploits TGF-β–induced processes such as EMT and increased invasive capacity to facilitate metastasis. Our data confirm that FTO, via upregulation of BUB1, amplifies TGF-β signaling, thus providing a mechanistic rationale for FTO's association with aggressive tumor characteristics and reduced patient survival.

Despite these compelling findings, certain limitations of this study should be acknowledged. Although our data demonstrate that FTO knockdown enhances m6A modification of BUB1 mRNA, the specific m6A sites on BUB1 mRNA remain unmapped. Additionally, the therapeutic implications of targeting the FTO–BUB1 axis warrant further exploration. Experiments using xenograft models with FTO-overexpressing cells and BUB1 knockdown could further validate this approach. Given that FTO ablation significantly restricted tumor growth in our xenograft assays, pharmacological inhibitors of FTO, in combination with existing targeted drugs or immunotherapies, may be an attractive strategy for advanced HCC. However, the potential systemic effects of FTO blockade, given FTO's roles in physiological metabolism and adipogenesis, will need careful evaluation.

Conclusions

This study highlights the critical function of FTO in orchestrating m6A-dependent regulation of BUB1 and the subsequent amplification of TGF-β signaling in HCC. By revealing how FTO-driven BUB1 upregulation fosters malignant phenotypes, specifically enhancing proliferation, EMT, and tumor invasiveness, our work offers new perspectives for targeting epitranscriptomic modifications in liver cancer. Further research on FTO inhibitors (e.g., FB23-2, Meclofenamate Sodium, Rhein, and Dac51), along with detailed characterization of the BUB1–TGF-βR1 axis, could yield novel therapeutic strategies to abrogate HCC progression and improve patient survival.

Funding

This work was supported by the National Natural Science Foundation of China (grant no. 82173360), the Chongqing Science and Health Joint Medical Research Project (grant no. 2024QNXM053), the Chongqing Natural Science Foundation (grant no. CSTB2024NSCQ-MSX0403 and CSTB-2022NSCQ-MSX1644), the China Postdoctoral Science Foundation (grant no. 2022M720606), and special support for postdoctoral researchers from Chongqing (grant no. 2022CQBSHTB2064).

Conflict of interest

The authors have no conflict of interests related to this publication.

Author contributions

Study concept and design (LZ, LG, ZM, SL), acquisition of data (LZ, LG, YL), analysis and interpretation of data (LZ, LG, YL, SL), drafting of the manuscript (LZ, LG), critical revision of the manuscript for important intellectual content (YL, ZM, SL), administrative, technical, or material support (ZM, SL), and study supervision (ZM, SL). All authors have made a significant contribution to this study and have approved the final manuscript.

Ethical statement

Written informed consent was obtained from all participants, and this study was approved by the Ethics Committee of The Second Affiliated Hospital of Chongqing Medical University (2021[152]).

Data sharing statement

The datasets generated and/or analyzed during the current study are available from the corresponding author upon reasonable request.

References

[1] Bo Z, Song J, He Q, Chen B, Chen Z, Xie X, *et al*. Application of artificial intelligence radiomics in the diagnosis, treatment, and prognosis of hepatocellular carcinoma. Comput Biol Med 2024;173:108337. doi:10.1016/j.compbiomed.2024.108337, PMID:38547656.

[2] Rich NE. Changing Epidemiology of Hepatocellular Carcinoma Within the United States and Worldwide. Surg Oncol Clin N Am 2024;33(1):1–12. doi:10.1016/j.soc.2023.06.004, PMID:37945136.

[3] Peiseler M, Schwabe R, Hampe J, Kubes P, Heikenwälder M, Tacke F. Immune mechanisms linking metabolic injury to inflammation and fibrosis in fatty liver disease - novel insights into cellular communication circuits. J Hepatol 2022;77(4):1136–1160. doi:10.1016/j.jhep.2022.06.012, PMID:35750137.

[4] Pinter M, Pinato DJ, Ramadori P, Heikenwalder M. NASH and Hepatocellular Carcinoma: Immunology and Immunotherapy. Clin Cancer Res 2023 ;29(3):513–520. doi:10.1158/1078-0432.CCR-21-1258, PMID:36166660.

[5] Wang X, Lu J. Immunotherapy for hepatocellular carcinoma. Chin Med J (Engl) 2024;137(15):1765–1776. doi:10.1097/CM9.0000000000003060, PMID:38855876.

[6] Yang X, Yang C, Zhang S, Geng H, Zhu AX, Bernards R, *et al*. Precision treatment in advanced hepatocellular carcinoma. Cancer Cell 2024;42(2):180–197. doi:10.1016/j.ccell.2024.01.007, PMID:38350421.

[7] Dai T, Li J, Ye L, Yu H, Deng M, Liu W, *et al*. Prognostic Role and Potential Mechanisms of N6-methyladenosine-related Long Noncoding RNAs in Hepatocellular Carcinoma. J Clin Transl Hepatol 2022;10(2):308–320. doi:10.14218/JCTH.2021.00096, PMID:35528973.

[8] Ouyang P, Li K, Xu W, Chen C, Shi Y, Tian Y, *et al*. METTL3 recruiting M2-type immunosuppressed macrophages by targeting m6A-SNAIL-CXCL2 axis to promote colorectal cancer pulmonary metastasis. J Exp Clin Cancer Res 2024;43(1):111. doi:10.1186/s13046-024-03035-6, PMID:38605400.

[9] Zhang C, Yu M, Hepperla AJ, Zhang Z, Raj R, Zhong H, *et al*. Von Hippel Lindau tumor suppressor controls m6A-dependent gene expression in renal tumorigenesis. J Clin Invest 2024;134(8):e175703. doi:10.1172/JCI175703, PMID:38618952.

[10] Chen D, Gu X, Nurzat Y, Xu L, Li X, Wu L, *et al*. Writers, readers, and erasers RNA modifications and drug resistance in cancer. Mol Cancer 2024;23(1):178. doi:10.1186/s12943-024-02089-6, PMID:39215288.

[11] Lin Y, Li J, Liang S, Chen Y, Li Y, Cun Y, *et al*. Pan-cancer Analysis Reveals m6A Variation and Cell-specific Regulatory Network in Different Cancer Types. Genomics Proteomics Bioinformatics 2024;22(4):qzae052. doi:10.1093/gpbjnl/qzae052, PMID:38970366.

[12] Zhang M, Yang C, Dong W, Zhao Y, Chen N, Gao C. Expression patterns and prognostic role of m6A RNA methylation regulators in Non-small Cell Lung Cancer. Cell Mol Biol (Noisy-le-grand) 2024;70(2):67–72. doi:10.14715/cmb/2024.70.2.11, PMID:38430042.

[13] Hua T, Zhang C, Fu Y, Qin N, Liu S, Chen C, *et al*. Integrative analyses of N6-methyladenosine-associated single-nucleotide polymorphisms (m6A-SNPs) identify tumor suppressor gene AK9 in lung cancer. Mol Carcinog 2024;63(3):538–548. doi:10.1002/mc.23669, PMID:38051288.

[14] Wang S, Zeng Y, Zhu L, Zhang M, Zhou L, Yang W, *et al*. The N6-methyladenosine Epitranscriptomic Landscape of Lung Adenocarcinoma. Cancer Discov 2024;14(11):2279–2299. doi:10.1158/2159-8290.CD-23-1212, PMID:38922581.

[15] Azzam SK, Alsafar H, Sajini AA. FTO m6A Demethylase in Obesity and Cancer: Implications and Underlying Molecular Mechanisms. Int J Mol Sci 2022;23(7):3800. doi:10.3390/ijms23073800, PMID:35409166.

[16] Liu Y, Liang G, Xu H, Dong W, Dong Z, Qiu Z, *et al*. Tumors exploit FTO-mediated regulation of glycolytic metabolism to evade immune surveillance. Cell Metab 2021;33(6):1221–1233.e11. doi:10.1016/j.cmet.2021.04.001, PMID:33910046.

[17] Chen A, Zhang VX, Zhang Q, Sze KM, Tian L, Huang H, *et al*. Targeting the oncogenic m6A demethylase FTO suppresses tumourigenesis and potentiates immune response in hepatocellular carcinoma. Gut 2024;74(1):90–102. doi:10.1136/gutjnl-2024-331903, PMID:38839271.

[18] Heinrich B, Cubero FJ. FTO/m6A/GPNMB axis: a novel promising target for hepatocellular carcinoma (HCC) treatment? Gut 2024;74(1):5–6. doi:10.1136/gutjnl-2024-332934, PMID:39089861.

[19] Jin T, Ding L, Chen J, Zou X, Xu T, Xuan Z, *et al*. BUB1/KIF14 complex promotes anaplastic thyroid carcinoma progression by inducing chromosome instability. J Cell Mol Med 2024;28(7):e18182. doi:10.1111/jcmm.18182, PMID:38498903.

[20] Cicirò Y, Ragusa D, Sala A. Expression of the checkpoint kinase BUB1 is a predictor of response to cancer therapies. Sci Rep 2024;14(1):4461. doi:10.1038/s41598-024-55080-y, PMID:38396175.

[21] Qiu J, Zhang S, Wang P, Wang H, Sha B, Peng H, *et al*. BUB1B promotes hepatocellular carcinoma progression via activation of the mTORC1 signaling pathway. Cancer Med 2020;9(21):8159–8172. doi:10.1002/cam4.3411, PMID:32977361.

[22] Ma L, Jiang J, Si Q, Chen C, Duan Z. IGF2BP3 Enhances the Growth of Hepatocellular Carcinoma Tumors by Regulating the Properties of Macrophages and CD8(+) T Cells in the Tumor Microenvironment. J Clin Transl Hepatol 2023;11(6):1308–1320. doi:10.14218/JCTH.2023.00184, PMID:37719968.

[23] Peng D, Fu M, Wang M, Wei Y, Wei X. Targeting TGF-β signal transduction for fibrosis and cancer therapy. Mol Cancer 2022;21(1):104. doi:10.1186/s12943-022-01569-x, PMID:35461253.

[24] Shi X, Yang J, Deng S, Xu H, Wu D, Zeng Q, *et al*. TGF-β signaling in the tumor metabolic microenvironment and targeted therapies. J Hematol Oncol 2022;15(1):135. doi:10.1186/s13045-022-01349-6, PMID:36115986.

[25] Massagué J. TGFbeta in Cancer. Cell 2008;134(2):215–230. doi:10.1016/j.cell.2008.07.001, PMID:18662538.

[26] Nyati S, Schinske-Sebolt K, Pitchiaya S, Chekhovskiy K, Chator A, Chaudhry N, *et al*. The kinase activity of the Ser/Thr kinase BUB1 promotes TGF-β signaling. Sci Signal 2015;8(358):ra1. doi:10.1126/scisignal.2005379, PMID:25564677.

[27] Felgner PL, Gadek TR, Holm M, Roman R, Chan HW, Wenz M, *et al*. Lipofection: a highly efficient, lipid-mediated DNA-transfection procedure. Proc Natl Acad Sci U S A 1987;84(21):7413–7417. doi:10.1073/pnas.84.21.7413, PMID:2823261.

[28] Cancer Genome Atlas Research Network. Comprehensive and Integrative Genomic Characterization of Hepatocellular Carcinoma. Cell 2017;169(7):1327–1341.e23. doi:10.1016/j.cell.2017.05.046, PMID:28622513.

[29] Love MI, Huber W, Anders S. Moderated estimation of fold change and dispersion for RNA-seq data with DESeq2. Genome Biol 2014;15(12):550. doi:10.1186/s13059-014-0550-8, PMID:25516281.

[30] Ishiyama M, Miyazono Y, Sasamoto K, Ohkura Y, Ueno K. A highly water-soluble disulfonated tetrazolium salt as a chromogenic indicator for NADH as well as cell viability. Talanta 1997;44(7):1299–1305. doi:10.1016/s0039-9140(97)00017-9, PMID:18966866.

[31] Franken NA, Rodermond HM, Stap J, Haveman J, van Bree C. Clonogenic assay of cells in vitro. Nat Protoc 2006;1(5):2315–2319. doi:10.1038/nprot.2006.339, PMID:17406473.

[32] Kleinman HK, Martin GR. Matrigel: basement membrane matrix with biological activity. Semin Cancer Biol 2005;15(5):378–386. doi:10.1016/j.semcancer.2005.05.004, PMID:15975825.

[33] Livak KJ, Schmittgen TD. Analysis of relative gene expression data using real-time quantitative PCR and the 2(-Delta Delta C(T)) Method. Methods 2001;25(4):402–408. doi:10.1006/meth.2001.1262, PMID:11846609.

[34] Mahmood T, Yang PC. Western blot: technique, theory, and trouble shooting. N Am J Med Sci 2012;4(9):429–434. doi:10.4103/1947-2714.100998, PMID:23050259.

[35] Lin JS, Lai EM. Protein-Protein Interactions: Co-Immunoprecipitation. Methods Mol Biol 2017;1615:211–219. doi:10.1007/978-1-4939-7033-9_17, PMID:28667615.

[36] Peritz T, Zeng F, Kannanayakal TJ, Kilk K, Eiríksdóttir E, Langel U, *et al*. Immunoprecipitation of mRNA-protein complexes. Nat Protoc 2006;1(2):577–580. doi:10.1038/nprot.2006.82, PMID:17406284.

[37] Ross J. mRNA stability in mammalian cells. Microbiol Rev 1995;59(3):423–450. doi:10.1128/mr.59.3.423-450.1995, PMID:7565413.

[38] Dominissini D, Moshitch-Moshkovitz S, Schwartz S, Salmon-Divon M, Ungar L, Osenberg S, *et al*. Topology of the human and mouse m6A RNA methylomes revealed by m6A-seq. Nature 2012;485(7397):201–206. doi:10.1038/nature11112, PMID:22575960.

[39] Donaldson JG. Immunofluorescence Staining. Curr Protoc Cell Biol 2015;69:4.3.1–4.3.7. doi:10.1002/0471143030.cb0403s69, PMID:26621373.

[40] Tomayko MM, Reynolds CP. Determination of subcutaneous tumor size in athymic (nude) mice. Cancer Chemother Pharmacol 1989;24(3):148–154. doi:10.1007/BF00300234, PMID:2544306.

[41] Safri F, Nguyen R, Zerehpooshnesfchi S, George J, Qiao L. Heterogeneity of hepatocellular carcinoma: from mechanisms to clinical implications. Cancer Gene Ther 2024;31(8):1105–1112. doi:10.1038/s41417-024-00764-w, PMID:38499648.

[42] Wang J, Wang F, Wang N, Zhang MY, Wang HY, Huang GL. Diagnostic and Prognostic Value of Protein Post-translational Modifications in Hepatocellular Carcinoma. J Clin Transl Hepatol 2023;11(5):1192–1200. doi:10.14218/JCTH.2022.00006S, PMID:37577238.

[43] Uddin MB, Wang Z, Yang C. Epitranscriptomic RNA m(6)A Modification in Cancer Therapy Resistance: Challenges and Unrealized Opportunities. Adv Sci (Weinh) 2024;12(4):e2403936. doi:10.1002/advs.202403936, PMID:39661414.

[44] Huang C, Chen W, Wang X. Studies on the fat mass and obesity-associated (FTO) gene and its impact on obesity-associated diseases. Genes Dis 2023;10(6):2351–2365. doi:10.1016/j.gendis.2022.04.014, PMID:37554175.

[45] Li Y, Su R, Deng X, Chen Y, Chen J. FTO in cancer: functions, molecular mechanisms, and therapeutic implications. Trends Cancer 2022;8(7):598–614. doi:10.1016/j.trecan.2022.02.010, PMID:35346615.

[46] Chen J, Du B. Novel positioning from obesity to cancer: FTO, an m(6)A RNA demethylase, regulates tumour progression. J Cancer Res Clin Oncol 2019;145(1):19–29. doi:10.1007/s00432-018-2796-0, PMID:30465076.

[47] Niu Y, Lin Z, Wan A, Chen H, Liang H, Sun L, *et al*. RNA N6-methyladenosine demethylase FTO promotes breast tumor progression through inhibiting BNIP3. Mol Cancer 2019;18(1):46. doi:10.1186/s12943-019-1004-4, PMID:30922314.

[48] Lin Z, Wan AH, Sun L, Liang H, Niu Y, Deng Y, *et al*. N6-methyladenosine demethylase FTO enhances chemo-resistance in colorectal cancer through SIVA1-mediated apoptosis. Mol Ther 2023;31(2):517–534. doi:10.1016/j.ymthe.2022.10.012, PMID:36307991.

[49] Yang S, Wei J, Cui YH, Park G, Shah P, Deng Y, *et al*. m(6)A mRNA demethylase FTO regulates melanoma tumorigenicity and response to anti-PD-1 blockade. Nat Commun 2019;10(1):2782. doi:10.1038/s41467-019-10669-0, PMID:31239444.

[50] Wang JY, Lu AQ. The biological function of m6A reader YTHDF2 and its role in human disease. Cancer Cell Int 2021;21(1):109. doi:10.1186/s12935-021-01807-0, PMID:33593354.

[51] Kim T, Gartner A. Bub1 kinase in the regulation of mitosis. Anim Cells Syst (Seoul) 2021;25(1):1–10. doi:10.1080/19768354.2021.1884599, PMID:33717411.

[52] Wang K, Shen K, Wang J, Yang K, Zhu J, Chen Y, *et al*. BUB1 potentiates gastric cancer proliferation and metastasis by activating TRAF6/NF-κB/FGF18 through m6A modification. Life Sci 2024;353:122916. doi:10.1016/j.lfs.2024.122916, PMID:39025206.

[53] Fujibayashi Y, Isa R, Nishiyama D, Sakamoto-Inada N, Kawasumi N, Yamaguchi J, *et al*. Aberrant BUB1 Overexpression Promotes Mitotic Segregation Errors and Chromosomal Instability in Multiple Myeloma. Cancers (Basel) 2020;12(8):2206. doi:10.3390/cancers12082206, PMID:32781708.